

Calculation of Frequency-Dependent S-Parameters of CPW Air-Bridges Considering Finite Metallization Thickness and Conductivity

Hang Jin and Ruediger Vahldieck

Laboratory for Lightwave Electronics, Microwaves and Communications
(LLiMiC)
Department of Electrical and Computer Engineering, University of Victoria
Victoria, B.C., V8W 3P6, Canada

ABSTRACT

Two types of CPW air-bridges are studied using the new full-wave frequency-domain TLM method. The finite thickness and conductivity of the air-bridge metallization, including superconductivity, is taken into account. Air-bridge s-parameters are presented for varying dimensions. Furthermore, cascading air-bridges and CPW discontinuities is investigated to determine the degree of interaction possible.

1. INTRODUCTION

Coplanar waveguides (CPW) are attractive transmission line structures for monolithic microwave integrated circuits (MMIC)[1]~[4]. CPW's exhibit not only low dispersion but provide also for easy implementation of active devices. To suppress the unwanted (even) mode in a CPW, either via holes or air-bridges are used to connect the uniplanar groundplane left and right from the center conductor. In a number of applications, however, a backmetallization can not be applied and therefore via holes are useless. In these cases air-bridges are the only way to connect the uniplanar groundplane. Two different kind of air-bridges are used. Both are shown in Fig.1. In type A, the groundplane is bridged over the center conductor. In type B, the center conductor is bridged over the groundplane. Since air-bridges represent discontinuities, their parasitic effects must be known for accurate circuit design.

In this paper we investigate the frequency-dependent s-parameters of air-bridges by using the frequency domain TLM method. This is a powerful new full-wave technique explained elsewhere, which can be applied for the s-parameter analysis of arbitrarily shaped guided wave discontinuities. The analysis presented here takes into account the finite thickness and conductivity of the air-bridge metallization and also that of the transmission line conductors. Since superconductors can be

considered as well, s-parameters for high-Tc superconductor air-bridges are given as an example to demonstrate the potential of this new method. This is the first time that the conductor losses are included in a full-wave analysis of air-bridge effects. S-parameters are given for air-bridges at 40GHz and varying dimensions like air-bridge height, length, metallization thickness and losses. We investigate also the influence of air-bridges located in the close vicinity of a CPW center conductor discontinuity. This is an interesting problem for high density circuits and an investigation has not been reported in the literature yet.

2. METHOD

The analysis is based on the new frequency-domain TLM (FDTLM) method which operates directly in the frequency domain while following the basic time domain TLM solution procedure. The method is explained in more detail in [5]. The FDTLM discretizes the space analyzed by the same transmission line network as the conventional TLM method, but employs a novel excitation which is an impulse sequence with its magnitude modulated by a sinusoidal wave. At any time step, this new excitation retains the form of an impulse but its modulated amplitude envelope contains the information of the structure at the modulation frequency. This new method has both the flexibility of the conventional TLM and the computational efficiency of frequency domain techniques, and is particularly suitable for structures with complicated geometries such as CPW air bridges.

3. NUMERICAL RESULTS

Before calculating the s-parameters for the air-bridges, we first analyze a simple in-line microstrip gap discontinuity and compare with experimental data from the literature to check the method[6]. The excellent agreement is shown in Fig.2. The convergence of the computation was checked by comparing the results with different TLM mesh

layouts. The results with $n_x=12$, $n_y=5$; $n_x=16$, $n_y=7$; and $n_x=20$, $n_y=7$ for air bridge type A are shown in Fig.3. Here n_x and n_y , respectively, are the number of nodes in transverse x- and y-directions. The length of the air bridge in z-direction is much smaller than 1/10 of the wavelength we are interested in. Therefore, only one node is needed for the z-direction. It should be mentioned that this new method allows to place the reference plane just into the discontinuity plane. Thus, only the air bridge area needs to be discretized for the s-parameter calculations. It is found that as the number of node increases from $16 \times 7 = 112$ to $20 \times 7 = 140$, the results are almost unchanged. In the following calculation a mesh layout with $n_x=16$, $n_y=7$ is used.

Fig.4 shows a comparison between S_{11} of air-bridges of both types with metal thickness of $t=0$ and $t=3\mu\text{m}$. It is found that the reflections coefficient for air bridges with finite metallization thickness are only marginally higher than those with zero thickness and that the type B air-bridge is slightly more sensitive. The marginal effect of the metallization thickness is plausible considering that the air-bridge behaves basically as a parasitic capacitor connecting in parallel with the main transmission line. One part of the capacitance comes from the parallel plane capacitor between the bottom plane of the air-bridge and the top plane of the center conductor. This part is almost independent from the thickness of the metallization. The other part results from the fringing fields at the ends of the air bridge and the gap of the CPW. This part of the capacitance will increase with the metallization thickness, but plays only a minor role.

It has been demonstrated that high- T_c superconductor has a prospective application in CPW structures to reduce the insertion losses[7]. The characteristics of the superconductor can be incorporated in the calculations via the two-fluid model where a superconductor is described as a dielectric medium with the complex conductivity[7]:

$$\sigma_{\text{super}} = \sigma_n (T/T_c)^4 - j(1 - (T/T_c)^4) / \omega \mu \lambda_0^2 \quad \text{for } T < T_c$$

where σ_n is the normal conductivity, T is the absolute temperature, and λ_0 is the zero-temperature penetration depth. Fig.5 shows the reflection coefficients for a superconductor air-bridge. In comparison to normal conductor conductivities, the effect of superconductors on the s-parameters is quite small and the differences between the results of superconductors and perfect

conductors are nearly invisible.

Fig's 6 and 7 illustrate the effect of air-bridge height and length on S_{11} . Both parameters seem to have an opposite effect on the phase in the different air-bridges, while the tendency on $|S_{11}|$ is the same. Finally Fig.8 demonstrates that there is very little interaction between the location of the CPW discontinuity air-bridge of type A. The change in the phase is due to the change in the length of the transmission line between both discontinuities.

4. CONCLUSION

For the first time the frequency-dependent s-parameters of CPW air-bridges with finite thickness and conductivity of the metallization are presented. It was found that the two types of air-bridges investigated have very little reflection and that metal losses have no significant effect on their performance. Further investigation on the effects of the bridge height and length as well as discontinuities in the air-bridge structure itself, which is important when bridging three-ports, are still on-going.

References

- [1] T.Hirota, Y.Tarusawa, and H.Ogawa, " Uniplanar MMIC Hybrids - A Proposed New MMIC Structure", IEEE Trans. Microwave Theory Tech., Vol.MTT-35, 1987, pp.576-581
- [2] N.H.L.Korter, S.Kosslowski, R.Bertenbury, S.Heinen, and I.Wolff, " Investigation On Air Bridges Used for MMICs in CPW Technique," Proc. European Microwave Conf.(1989) London, pp.666-671
- [3] K.Beilenhoff, W.Heinrich, and H.L.Hartnagel, " The Scattering Behavior of Air Bridges in Coplanar MMICs", Proc. European Microwave Conf.(1991) Stuttgart, pp.1131-1135
- [4] N.I.Dib, P.B.Katehi, and G.E.Ponchak, " Analysis of Shield CPW Discontinuities with Air-bridges", 1991 IEEE MTT-S Inter. Microwave Symp. Digest, Boston, pp.469-472
- [5] H.Jin and R.Vahldieck, " A Frequency Domain TLM Method", 1992 IEEE MTT-S Inter. Microwave Conf., Albuquerque, NM
- [6] M.Drissi, F.Hanna, and J.Citerne, " Theoretical and Experimental investigations of Open Microstrip Gap Discontinuities", Proc. European Microwave Conf.(1988) Stockholm, Sweden
- [7] W.Chew, A.L.Riley, D.L.Rascoe, B.D.Hunt, M.C.Foote, T.W.Cooley, and L.J.Bajuk, " Design and Performance of a High- T_c Superconductor Coplanar Waveguide Filter", IEEE Trans. Microwave Theory Tech., Vol.MTT-39, 1991, pp.1455-1461

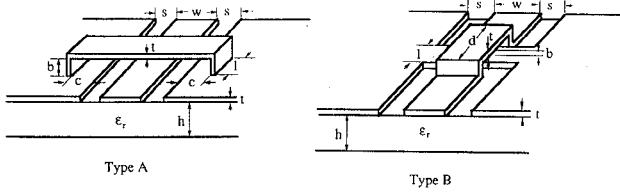


Fig.1 Two types of CPW air-bridges under consideration

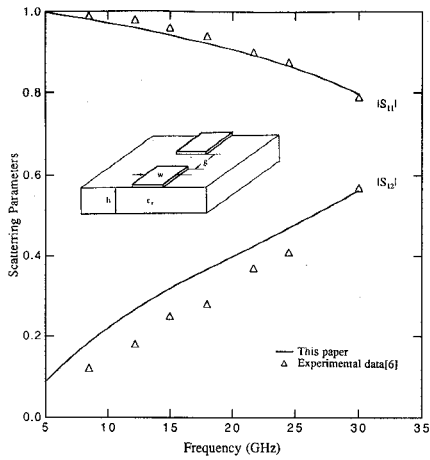


Fig.2 Frequency-dependent S-parameters for a microstrip gap discontinuity ($w=0.635$ mm, $h=w$, $g=0.35h$, $\epsilon_r=9.9$)

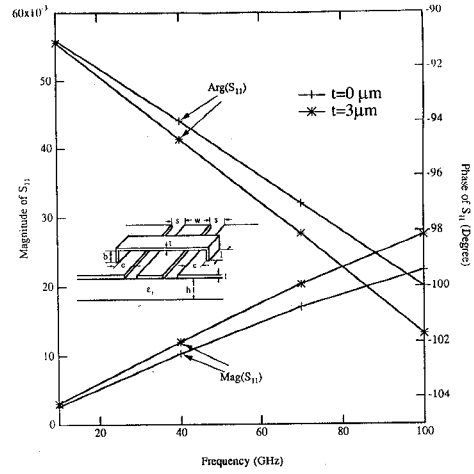


Fig.4 Frequency-dependent reflection coefficients for CPW air-bridges with two different metallization thickness $t=0$ and $t=3\mu\text{m}$ ($w=15\mu\text{m}$, $s=10\mu\text{m}$, $b=3\mu\text{m}$, $l=30\mu\text{m}$, $d=45\mu\text{m}$, $c=0$, $h=100\mu\text{m}$, $\epsilon_r=12.9$)

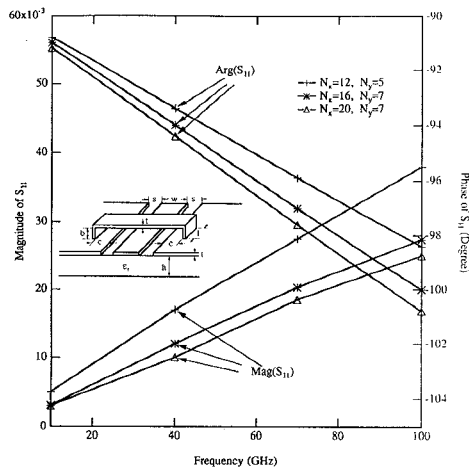
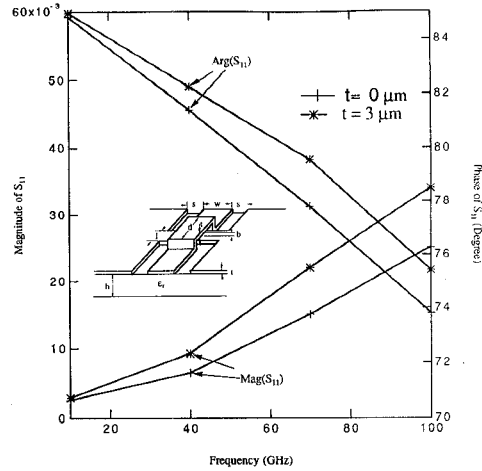


Fig.3 Frequency-dependent reflection coefficients for air bridge type A with different TLM mesh layouts ($w=15\mu\text{m}$, $s=10\mu\text{m}$, $b=3\mu\text{m}$, $l=30\mu\text{m}$, $c=0$, $h=100\mu\text{m}$, $t=3\mu\text{m}$, $\epsilon_r=12.9$)

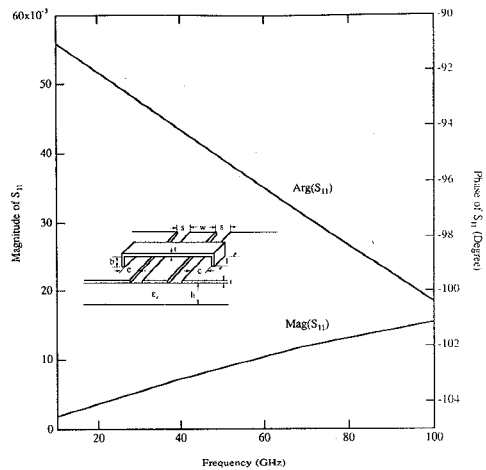


Fig.5 Frequency dependent reflection coefficients for a superconducting CPW air-bridge (YBCO: $T_c=92.5\text{K}$, $T=77\text{K}$, $\sigma_{11}=1700\text{s/mm}$, $\lambda=0.3\text{nm}$, $w=15\mu\text{m}$, $s=10\mu\text{m}$, $b=3\mu\text{m}$, $l=30\mu\text{m}$, $c=0$, $h=100\mu\text{m}$, $t=3\mu\text{m}$, $\epsilon_r=12.9$)

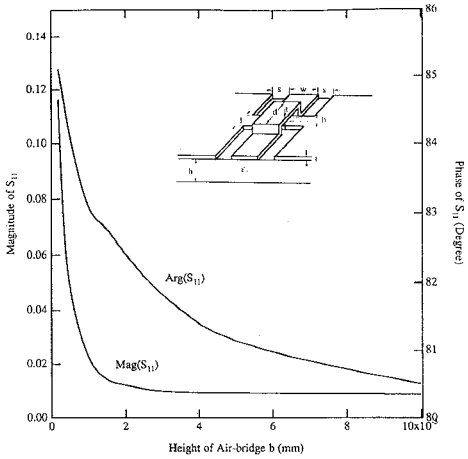
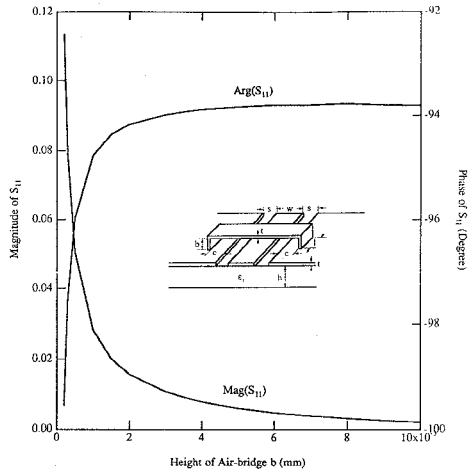


Fig.6 Reflection coefficients for CPW air bridges versus the height of the air bridges at frequency 40 GHz ($w=15\mu\text{m}$, $s=10\mu\text{m}$, $l=30\mu\text{m}$, $d=45\mu\text{m}$, $c=0$, $h=100\mu\text{m}$, $t=3\mu\text{m}$, $\epsilon_r=12.9$)

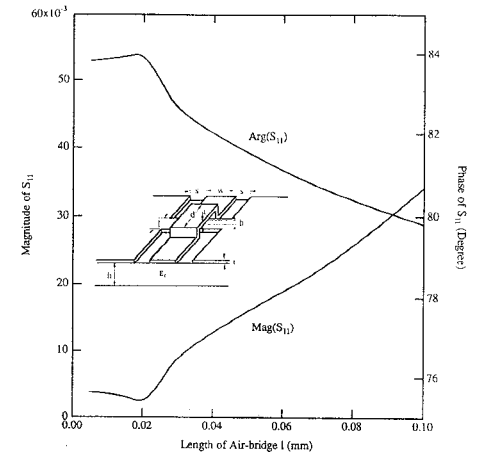
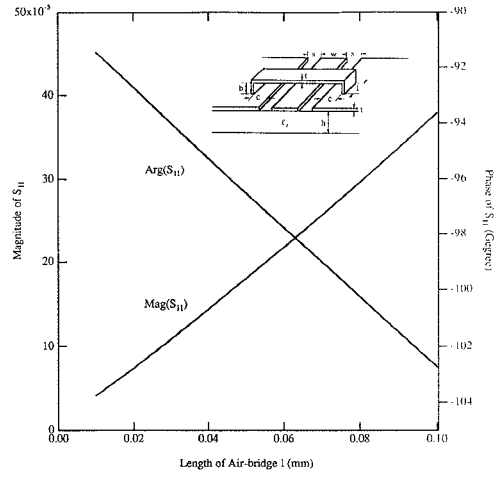


Fig.7 Reflection coefficients for CPW air bridges versus the length of the air bridges at frequency 40 GHz ($w=15\mu\text{m}$, $s=10\mu\text{m}$, $b=3\mu\text{m}$, $d=15\mu\text{m}$, $c=0$, $h=100\mu\text{m}$, $t=3\mu\text{m}$, $\epsilon_r=12.9$)

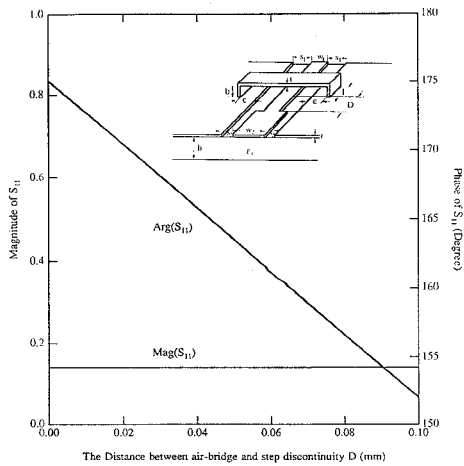


Fig.8 Reflection coefficients for a combination of CPW air bridge and step discontinuity versus the distance between air-bridge and step discontinuity at frequency 40GHz ($w_1=12\mu\text{m}$, $w_2=20\mu\text{m}$, $s_1=12\mu\text{m}$, $s_2=8\mu\text{m}$, $l=30\mu\text{m}$, $b=3\mu\text{m}$, $c=0$, $h=100\mu\text{m}$, $t=3\mu\text{m}$, $\epsilon_r=12.9$)